Available online at www.sciencedirect.com

SciVerse ScienceDirect

Ceramics International 38 (2012) 2381–2387

CERAMICS INTERNATIONAL

www.elsevier.com/locate/ceramint

Mechanical properties and microstructure of porous BN–SiO_2–Si_3N_4 composite ceramics

Na-Na Long [a,b], Jian-Qiang Bi [a,b,c,*], Wei-Li Wang [a,b], Ming Du [a,b], Yu-Jun Bai [a]

[a] Key Laboratory for Liquid–Solid Structural Evolution and Processing of Materials, Ministry of Education, Shandong University, Jinan 250061, PR China
[b] Engineering Ceramics Key Laboratory of Shandong Province, Shandong University, Jinan 250061, PR China
[c] Faculty of Engineering, Department of Physics and Astronomy, and Nanoscience and Engineering Center, University of Georgia, Athens, GA 30602, USA

Received 25 May 2011; received in revised form 31 October 2011; accepted 2 November 2011
Available online 7 November 2011

Abstract

Porous silicon nitride (Si_3N_4) ceramics incorporated with hexagonal boron nitride (h-BN) and silica (SiO_2) nanoparticles were fabricated by pressureless-sintering at relatively low temperature, in which stearic acid was used as pore-making agent. Bending strength at room and high temperatures, thermal shock resistance, fracture toughness, elastic modulus, porosity and microstructure were investigated in detail. The mechanical properties and thermal shock resistance behavior of porous Si_3N_4 ceramics were greatly influenced by incorporation of BN and SiO_2 nanoparticles. Porous BN–SiO_2–Si_3N_4 composites were successfully obtained with good critical thermal shock temperature of 800 °C, high bending strength (130 MPa at room temperature and 60 MPa at 1000 °C) and high porosity.

Keywords: B. Porosity; C. Thermal shock resistance; D. Si_3N_4; D. SiO_2

1. Introduction

Porous Si_3N_4 has become one of the hot topics for decades as functional components such as gas turbine, catalyst carriers and antenna windows due to its good dielectric properties, excellent oxidation resistance, high bending strength at room and elevated temperatures and excellent thermal shock resistance [1–4]. However, the relatively high thermal expansion coefficient limits its wider applications [2,5]. To solve this problem, it is desirable to reduce the thermal expansion coefficient of Si_3N_4. The incorporation of second phase with low thermal expansion coefficient is an effective method. According to the reported experimental results, BN and SiO_2 are good candidates. They both have good thermal shock resistance [6,7], low dielectric constant [4,8] as well as low thermal expansion coefficient. Moreover, BN–Si_3N_4 composites showed excellent machinability, improved fracture toughness and thermal shock resistance compared to monolithic Si_3N_4 ceramics [9,10]. SiO_2–Si_3N_4 composites also showed good mechanical properties and high thermal conductivity [4,11,12], which were reported in recent studies. Thus, it is reasonable to infer that the three-phase system of porous BN–SiO_2–Si_3N_4 composites will possess good mechanical properties, dielectric properties and low thermal expansion coefficient.

The fracture behavior of most dense ceramics is brittle fracture, and unexpected stress usually serves as the crack propagation dynamic. Porous ceramics have the same fracture behavior as the dense ones. Reduction of elastic modulus while retaining bending strength is an ideal method to avoid the abrupt failure of porous ceramics [13,14]. In view of this, high porosity and second phase with low elastic modulus are introduced to reduce elastic modulus. Compared to the constituents, composite has an intermediate elastic modulus value between upper and lower bounds according to the Voigt and Reuss models [15]. The elastic modulus decreases with the porosity by the following equation [16]:

$$E = E_0 \exp(-b\,p) \tag{1}$$

where E_0 is the elastic modulus at a porosity $p = 0$ and b is a material constant. However, pores inside the body inevitably

* Corresponding author at: Key Laboratory for Liquid–Solid Structural Evolution and Processing of Materials, Ministry of Education, Shandong University, Jinan 250061, PR China. Tel.: +86 531 88392439; fax: +86 531 88392315.
E-mail address: bjq1969@163.com (J.-Q. Bi).

0272-8842/$36.00.
doi:10.1016/j.ceramint.2011.11.003

deteriorate bending strength. The relationship between bending strength and porosity can be described as [16]:

$$\sigma_f = \sigma_0 \ \exp(-b\,p) \tag{2}$$

where σ_0 is the strength at a porosity $p = 0$ and b is a material constant. In addition, high porosity will also have influence on thermal shock resistance. However, porous ceramics with well pore-size distribution and high open porosity have many applications due to their excellent properties [17,18]. Therefore, it is desirable to control microstructure and pore distribution to balance strength, elastic modulus and thermal shock resistance of materials.

In our work, porous BN–SiO_2–Si_3N_4 composites were fabricated by pressureless sintering using stearic acid as pore-making agent at 1500 °C. The bending strength at room and high temperatures, elastic modulus, thermal shock behavior, pore-size distribution and microstructure were evaluated, and the dielectric properties will be discussed later.

2. Experimental

The samples in the experiment were fabricated by pressureless-sintering, α-Si_3N_4, h-BN, and SiO_2 as the starting powders, stearic acid as pore-forming agent, and Y_2O_3 and Al_2O_3 as sintering additives. The sample designation and mass fraction are listed in Table 1. The powders were ball-milled in distilled water for 6 h in a ball-milling tank. The slurry was dried in an oven and sieved through a 100-mesh screen. The mixtures were then weighed and uniaxially pressed into rectangular shape (40 mm × 40 mm × 4 mm) at a pressure of 40 MPa, in which polyvinyl alcohol (PVA) was incorporated as binder. The pressed green compacts were preheated in a muffle furnace up to 700 °C at a rate of 3 °C/min in air, and then placed in a graphite case and sintered in a multi-purpose high temperature furnace (High-Multi 5000, Fijidenpa Co. Ltd., Osaka, Japan) at 1500 °C under a circumstance of N_2. The heating rate was 10 °C/min, and holding time was 1 h.

The sintered bodies were polished and sliced to test bars with the dimensions of 3 mm × 4 mm × 40 mm for room (RT) and high (HT) temperature bending strength (σ_f) and thermal shock resistance test, 2 mm × 4 mm × 40 mm with a notch in the depth of ~2 mm in the middle for fracture toughness (K_{IC}) test, and 1.8 mm × 4 mm × 40 mm for elastic modulus (E) test. RT bending strength, K_{IC} and E test were conducted via the three-point bending method with a span of 20 mm, and the test speed was 0.5 mm/min for RT fracture and 0.05 mm/min for K_{IC} and E test. Water quench technique was adopted to determine the thermal shock behavior. The specimens were heated at temperatures ranging from 415 °C to 815 °C in a muffle furnace at a heating rate of 20 °C/min and kept for 20 min to obtain the homogenous temperature distribution, and then the heated testing bars were quenched in water of 15 °C immediately which corresponded to the thermal shock temperature differences of 400–800 °C. After that, the residual strength was also measured by three-point bending method. The strain tolerance of porous silicon nitride was expressed by the value of σ_f/E [13].

Table 1
Compositions of the starting powder mixtures.

Sample no.	Compositions (wt.%)		
	Si_3N_4 + Al_2O_3 + Y_2O_3 + stearic acid	BN	SiO_2
S1	100	0	0
S2	95	5	0
S3	90	10	0
S4	95	0	5
S5	90	0	10
S6	90	5	5
S7	85	10	5

The HT strength test bars inside the furnace were heated ranging from 600 °C to 1000 °C at the heating rate of 20 °C/min, and kept for an additional 20 min for thermal equilibrium. Then the three-point bending test was conducted with a span of 30 mm and the test speed of 0.5 mm/min.

All the mechanical testing was conducted using a universal testing machine (Shenzhen SANS Testing Machine Co., Ltd., Shenzhen, China) attaching a box furnace. Generally, more than five specimens of each sample were tested for each test.

The bulk density and open porosity of the sintered samples were measured by the Archimedes displacement method. The theoretical density (ρ_{th}) of the mixture was calculated according to the following formula:

$$\rho_{th} = \frac{m}{\sum m_i/\rho_i} \tag{3}$$

where m_i and ρ_i represent the weight and density of different components, m is the total weight of the mixture. The relative density (ρ_r) can be calculated from the difference between theoretical (ρ_t) and bulk density (ρ_b) [4]:

$$\rho_r = \frac{\rho_b}{\rho_t} \tag{4}$$

The total porosity can be obtained by the following equation:

$$P_t = 1 - \rho_r \tag{5}$$

Crystalline phases were identified by X-ray diffraction analysis (XRD, Dmax-rc, Rigaku, Japan). The fracture surfaces of the samples after testing were used for the SEM observation by scanning electron microscopy (SEM, Quanta FEG 250, FEI, USA).

3. Results and discussion

3.1. Densification and mechanical properties

The mechanical properties and porosity are listed in Table 2. Compared to monolithic porous Si_3N_4 ceramics, the BN–SiO_2–Si_3N_4 composites have good properties such as low elastic modulus, high strength, toughness and open porosity. In particular, S3 shows good strain tolerance, which is a parameter indicating the material stability [13]. The total porosity of S3 calculated according to Eq. (5) is approximately 40% while that of the monolithic porous Si_3N_4 is 35%. Additionally, the open

Table 2
Mechanical properties and relative density of samples.

Sample no.	σ_f (MPa)	P_t (%)	Open porosity (%)	E (GPa)	K_{IC} (MPa m$^{1/2}$)	Strain tolerance ($\times 10^{-3}$)
S1	207 ± 17	35	28	110	2.29 ± 0.11	1.88
S2	149 ± 6	41	32	81	2.10 ± 0.05	1.84
S3	114 ± 12	40	35	24	1.66 ± 0.03	4.75
S4	105 ± 1	43	37	57	1.49 ± 0.14	1.84
S5	95 ± 6	39	34	42	1.53 ± 0.04	2.26
S6	125 ± 13	41	37	66	1.76 ± 0.05	1.89
S7	130 ± 15	40	38	66	1.85 ± 0.12	1.97

porosity increases with increase of the content of BN or SiO_2. The main reason is that nano-particles homogenously disperse in Si_3N_4 to retard the liquid diffusion rate and mass transport, and finally more open pores are stacked among the particles.

The monolithic porous Si_3N_4 ceramics with porosity of 35% attains σ_f of 207 MPa, E of 110 GPa and K_{IC} of 2.29 MPa m$^{1/2}$. However, in spite of composites possess almost equivalent porosity as the monolith, σ_f, K_{IC} and E decrease with the increase of the content of BN or SiO_2. This is mainly ascribed to the weak interface between Si_3N_4 and the second phase and the higher interconnected pores that formed with the increase of BN and SiO_2.

3.2. Phase transformation and microstructures

The XRD patterns of monolithic porous Si_3N_4 and BN/SiO_2–Si_3N_4 composites are shown in Fig. 1. Peaks of α-Si_3N_4, β-Si_3N_4 and $Y_2Si_3O_3N_4$ are observed in monolithic Si_3N_4. Besides these, h-BN is observed in BN–Si_3N_4 composite, and Si_2N_2O, $Y_2Si_2O_7$, and cristobalite were detected when SiO_2 is incorporated. At a given temperature of 1500 °C, β-Si_3N_4, $Y_2Si_3O_3N_4$, $Y_2Si_2O_7$, Si_2N_2O and cristobalite form in the presence of a liquid phase. The presence of cristobalite will induce the formation of microcracks which may be the main reason for lower strength of SiO_2–Si_3N_4 ceramics than other Si_3N_4 matrix composites [7].

The fracture surfaces of the samples observed by SEM are shown in Fig. 2a–g. Through microstructure analysis, it can be observed that the samples consisted of bonded particles and minor columnar grains with high aspect ratio, indicating a few α/β phase transformations, and this is well consistent with the XRD analysis. It also can be seen that the pores distribute uniformly in the matrix, and the connected open pores are formed by stacking Si_3N_4 particles, as clearly shown in Fig. 2. Moreover, the high open porosity provides more space available to the formation of elongated grains, which is helpful to high bending strength. This is also the reason why porous Si_3N_4 matrix ceramics attain high strength and porosity.

3.3. Thermal shock resistance

The residual strength after water quench is measured to characterize the thermal shock resistance, as shown in Fig. 3. ΔT_c is defined as the critical thermal shock differential temperature which can be calculated by the following equation [19]:

$$\Delta T_c = \frac{\sigma_f(1-\nu)}{\alpha E} \tag{6}$$

where the ν is the Poisson's ration, α is the thermal expansion coefficient.

Therefore, reduction of α and increase of strain tolerances (σ_f/E) are efficient ways to improve thermal shock resistance.

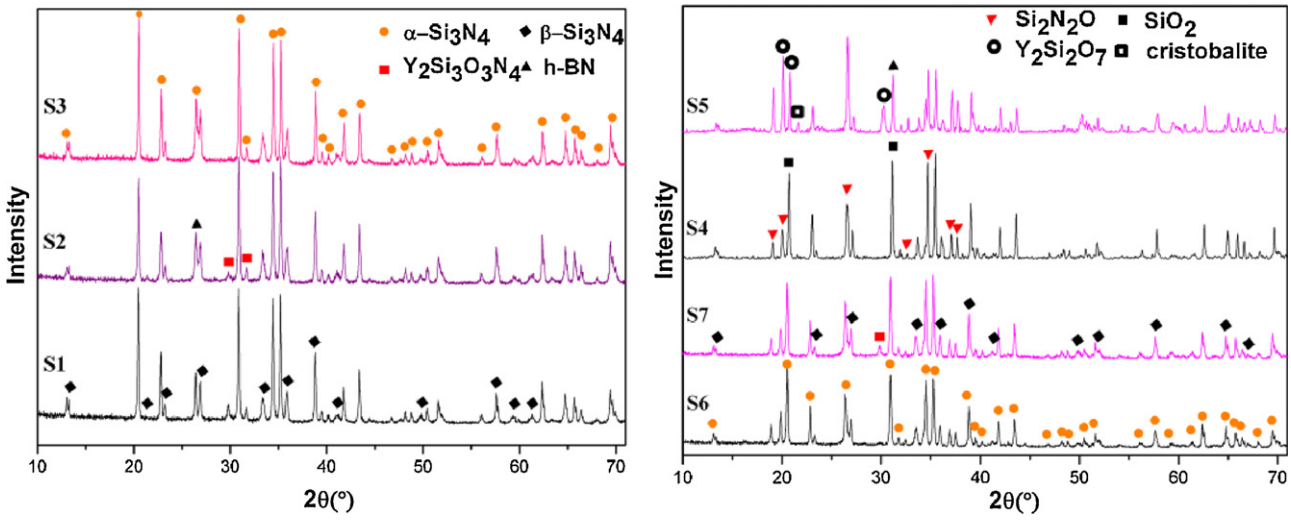

Fig. 1. XRD patterns of samples.

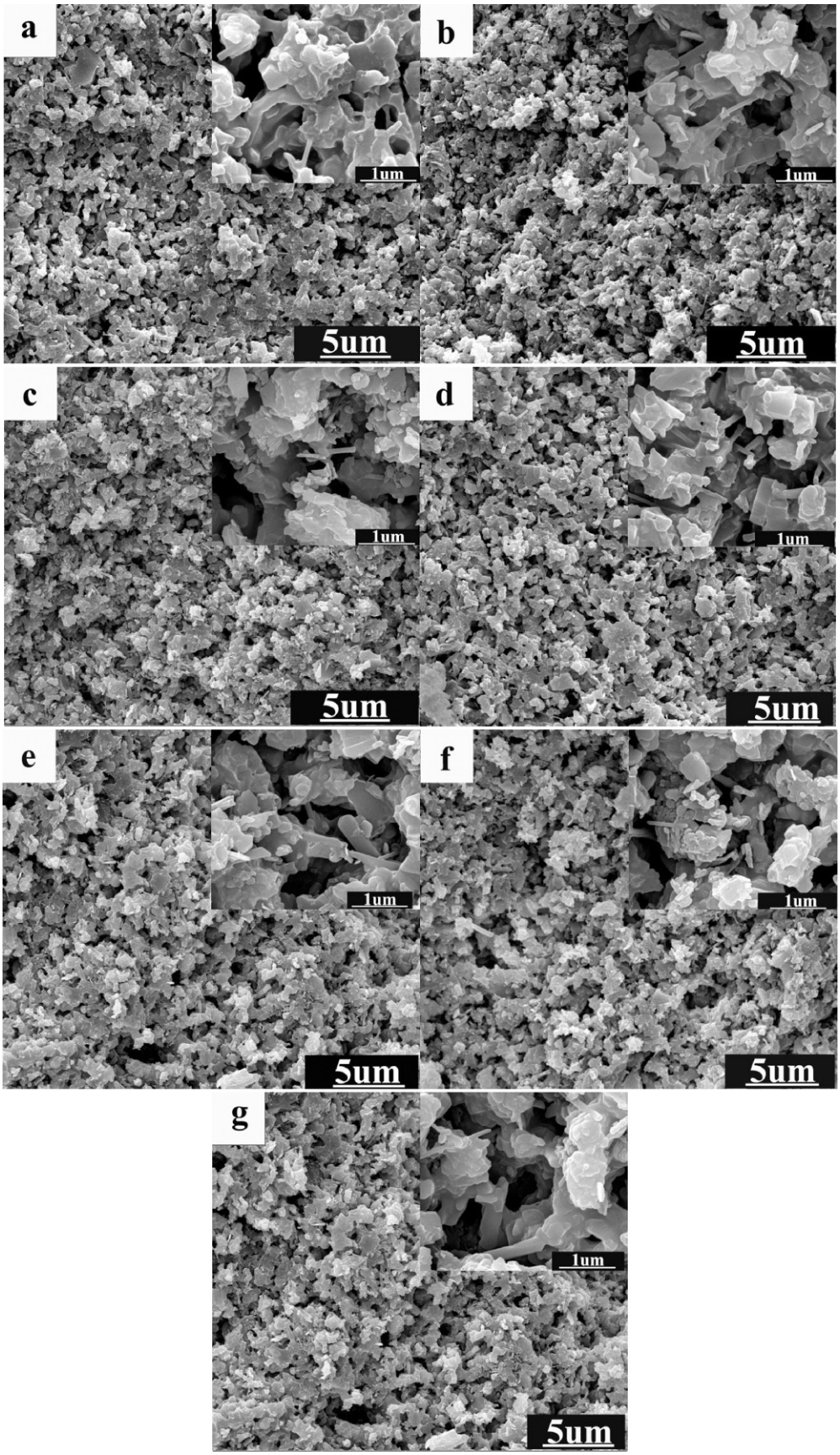

Fig. 2. Fracture surfaces of samples: (a) monolithic porous Si_3N_4 ceramics; (b) 5 wt.% BN–Si_3N_4 composites; (c) 10 wt.% BN–Si_3N_4 composites; (d) 5 wt.% SiO_2–Si_3N_4 composites; (e) 10 wt.% SiO_2–Si_3N_4 composites; (f) 5 wt.% BN-5 wt.%SiO_2–Si_3N_4 composites; (g) 10 wt.% BN–5 wt.%SiO_2–Si_3N_4 composites.

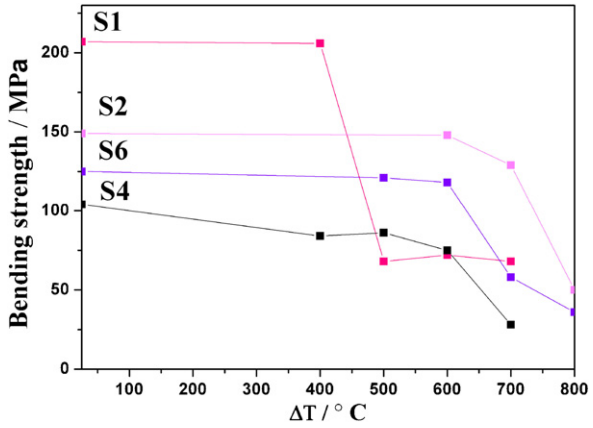

Fig. 3. Bending strength of porous Si_3N_4 matrix composites as a function of thermal shock temperature difference (ΔT).

The tensile thermal stress (σ_t) is generated when materials undergo rapid heating and quenching, which can be estimated by the following formula [19]:

$$\sigma_t = \frac{\alpha E}{1-\nu}\Delta T \tag{7}$$

where ΔT is the quench temperature difference.

The failure would happen when σ_t exceeds σ_f. So reduction of E is an available way to keep certain ceramic reliable with the same temperature difference according to Eq. (7).

Generally, porous ceramics, especially with connected open pores, possess good thermal shock resistance, because the pores can promote the reduction of stress concentration [14,20]. We can see that S1 shows an abrupt decrease after thermal shock with temperature difference of 400 °C while other three samples showed gradual reduction after 600 °C from Fig. 3. The reason for the poor thermal shock resistance of S1 is that higher elastic modulus induces higher tensile thermal stress as to the same temperature difference. And the excellent thermal

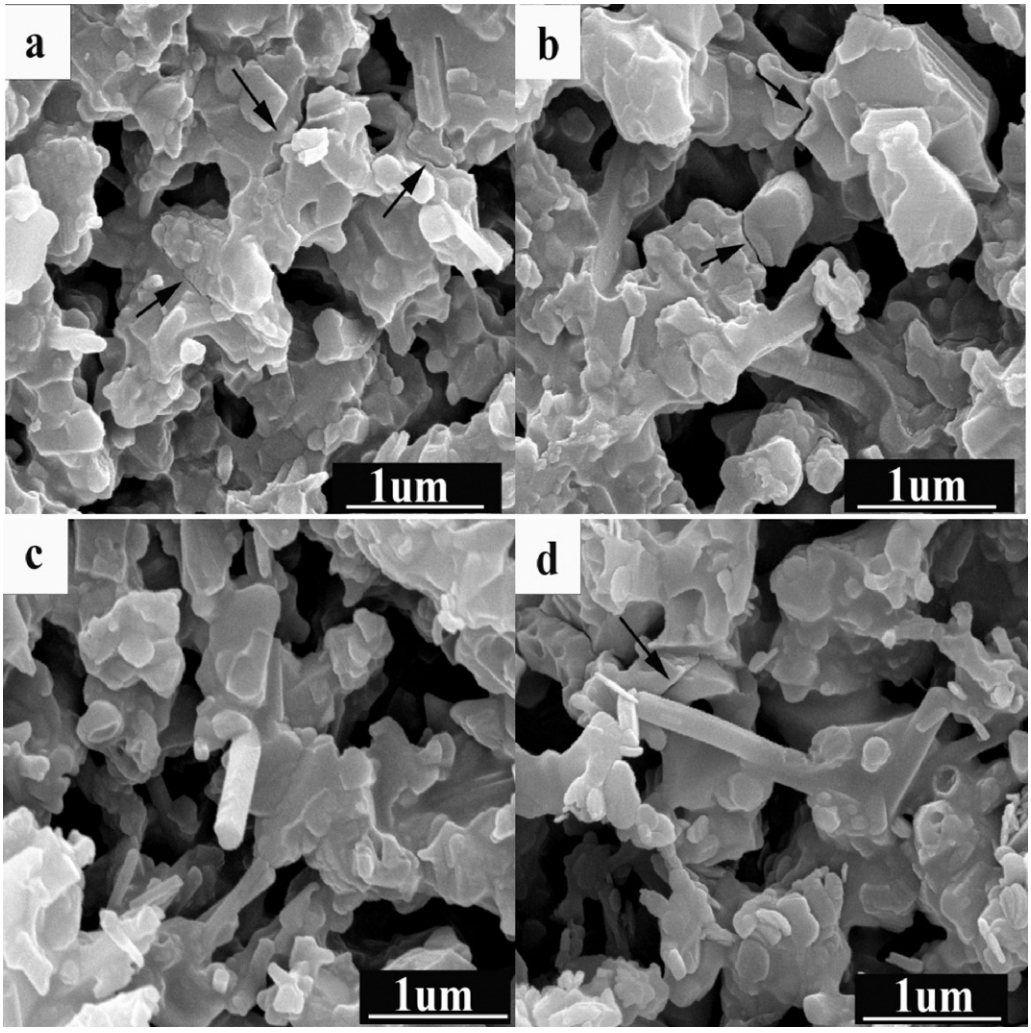

Fig. 4. SEM observations of fracture surfaces of porous Si_3N_4 matrix composites after thermal shock: (a) monolithic Si_3N_4 ceramics after thermal shock temperature difference of 700 °C; (b) 5 wt.% BN–Si_3N_4 composites after thermal shock temperature difference of 800 °C; (c) 5 wt.% SiO_2–Si_3N_4 composites after thermal shock temperature difference of 700 °C; (d) 5 wt.% BN–5 wt.%SiO_2–Si_3N_4 composites after thermal shock temperature difference of 800 °C.

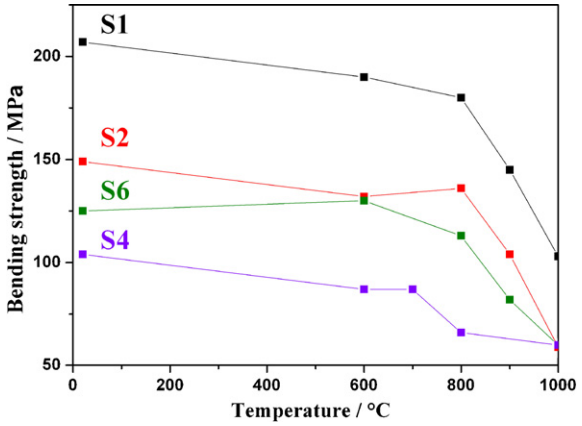

Fig. 5. Bending strength of porous Si_3N_4 matrix composites as a function of temperature.

shock resistance of BN–SiO_2–Si_3N_4 composites is probably benefited from low coefficient of thermal expansion of BN and SiO_2, high strain to failure and connected open pores. The surface morphologies of the samples after thermal shock test are shown in Fig. 4. It can be found that cracks exist among grains and their propagation ceases once they meet pores as indicted by the arrows in Fig. 4. These cracks probably originate due to the interactions between thermal stress and weak interfacial bonding forces among grains. Comparing fracture surfaces before and after thermal shock shown in Figs. 2 and 4, it can be concluded that the fracture mode at room temperature may be intergranular fracture while transgranular fracture after water quenching, which is similar to the fracture behavior of dense ceramics before and after thermal shock test.

3.4. High-temperature strength

The bending strength as a function of temperature is shown in Fig. 5. It can be observed that the strength decreases slowly until 800 °C and then drops fast. As reported, the deterioration at high temperature is caused by softening of the grain boundary glassy phase and consequent grain boundary sliding and cavitation [21,22], which hardly happens at low temperature. Therefore, the composites maintain original strength in a certain range of temperatures. However, when

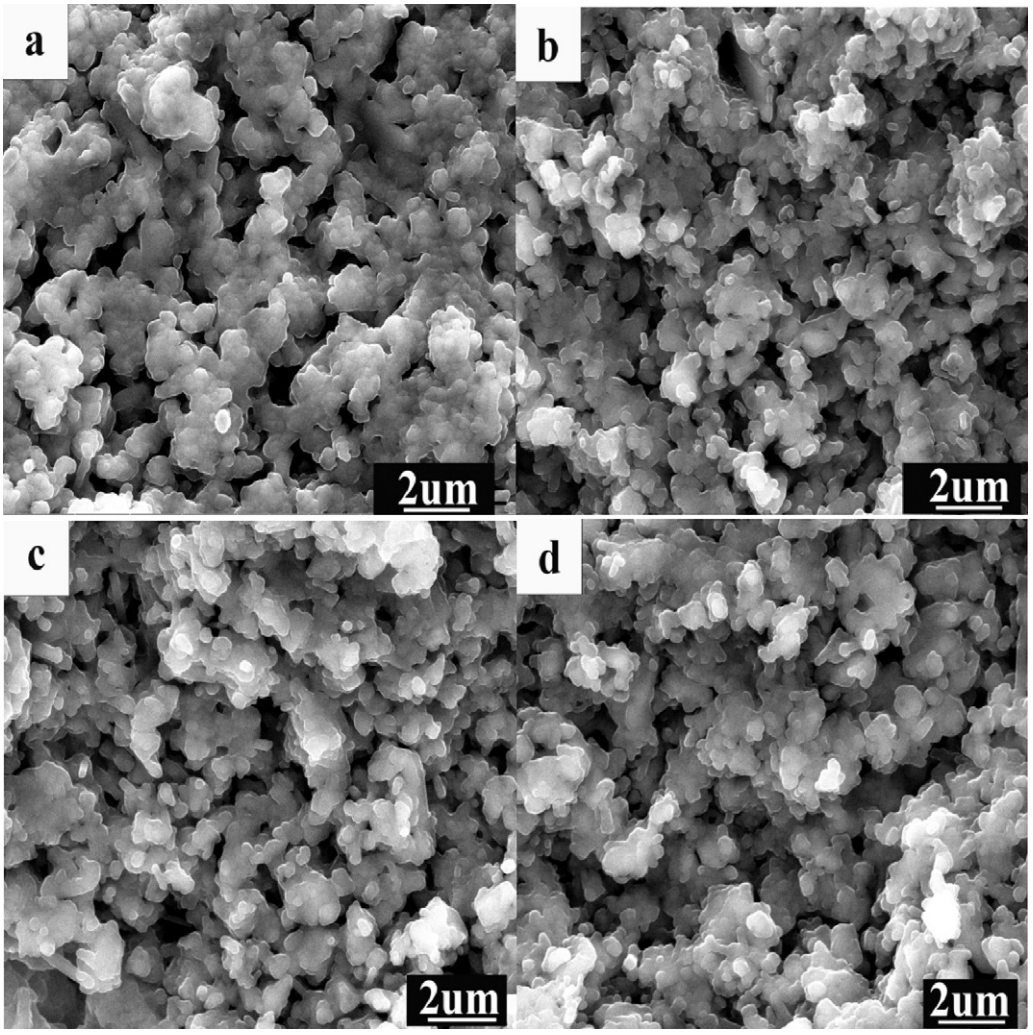

Fig. 6. SEM micrographs of porous Si_3N_4 matrix composites fractured at 1000 °C: (a) monolithic Si_3N_4 ceramics; (b) 5 wt.% BN–Si_3N_4 composites; (c) 5 wt.% SiO_2–Si_3N_4 composites; (d) 5 wt.% BN–5 wt.% SiO_2–Si_3N_4 composites.

temperature continues to increase, the grain boundary glassy will soften, and grain boundary sliding and cavitation will take place. The SEM images after high-temperature strength test are shown in Fig. 6. It can be seen that the fracture surfaces become viscous compared to those of samples fractured at room temperature (Fig. 2). It is probably caused by the softening of glass phase, which is also the main reason for strength degradation in the testing temperature range in this study. Moreover, the weak interface between glass phases and grains is also one of the factors that cause the failure at elevated temperatures.

4. Conclusions

Porous BN–SiO_2–Si_3N_4 composites were fabricated by pressureless-sintering at 1500 °C. The composites with porosity of 40% show high bending strength of 130 MPa and low elastic modulus of 66 GPa.

The thermal shock resistance of the composites is improved due to low coefficient of thermal expansion of BN and SiO_2, high strain tolerance and connected open pores.

The HT bending strength of porous Si_3N_4 composites is stable until the temperature reaches 800 °C. Softening of the grain boundary glassy phase as well as weak interface leads to strength degradation with increasing temperature.

Acknowledgements

This work is supported by the National Natural Science Foundation of China (No. 50872072, 51042005, and 50972076), Development Project of Shandong Province (2011GGX10205), Independent Innovation Foundation of Shandong University (2009TS001) and Graduate Independent Innovation Foundation of Shandong University (31370070613213).

References

[1] S.Y. Shan, J.F. Yang, Porous silicon nitride ceramics prepared by reduction–nitridation of silica, J. Am. Ceram. Soc. 88 (2005) 2594–2596.
[2] J.F. Feng, T. Ohji, Microstructure and mechanical properties of silicon nitride ceramics with controlled porosity, J. Am. Ceram. Soc. 85 (2002) 1512–1516.
[3] S. Li, Y. Pei, Mechanical and dielectric properties of porous Si_2N_2O–Si_3N_4 in situ composites, Ceram. Int. 35 (2009) 1851–1854.
[4] X. Li, X. Yin, Mechanical and dielectric properties of porous Si_3N_4–SiO_2 composite ceramics, Mater. Sci. Eng. A 500 (2009) 63–69.
[5] R.G. Duan, G. Roebben, Thermal stability of situ formed Si_3N_4–Si_2N_2O–TiN composites, J. Eur. Ceram. Soc. 22 (2002) 2527–2535.
[6] J. Eichler, C. Lesniak, Boron nitride (BN) and BN composites for high-temperature applications, J. Eur. Ceram. Soc. 28 (2008) 1105–1109.
[7] J.H. Wu, J.K. Guo, Preparation and properties of SiO_2 matrix composites doped with AlN particles, J. Mater. Sci. 35 (2000) 4895–4900.
[8] Y. Bo, J.X. Liu, Silicon nitride/boron nitride ceramic composites fabricated by reactive pressureless sintering, Ceram. Int. 35 (2009) 2155–2159.
[9] T. Kusunose, T. Sekino, Machinability of silicon nitride/boron nitride nanocomposite, J. Am. Ceram. Soc. 85 (2002) 2689–2695.
[10] E.H. Lutz, M.V. Swain, Fracture toughness and thermal shock behavior of silicon nitride–boron nitride ceramics, J. Am. Ceram. Soc. 75 (1992) 67–70.
[11] H. Miyazaki, Y.I. Yoshizawa, Fabrication of high thermal-conductive silicon nitride ceramics with low dielectric loss, Mater. Sci. Eng. B 161 (2009) 198–201.
[12] S. Ding, Y.P. Zeng, Oxidation bonding of porous silicon nitride ceramics with high strength and low dielectric constant, Mater. Lett. 61 (2007) 2277–2280.
[13] Y. Shigegaki, M.E. Brito, Strain tolerant porous silicon nitride, J. Am. Ceram. Soc. 80 (1997) 495–498.
[14] Y. Inagaki, T. Ohgi, Fracture energy of an aligned porous silicon nitride, J. Am. Ceram. Soc. 83 (2000) 1807–1809.
[15] T. Kusunose, T. Sekino, Fabrication and microstructure of silicon nitride/boron nitride nanocomposites, J. Am. Ceram. Soc. 85 (2002) 2678–2688.
[16] J.F. Yang, T. Ohji, Microstructure and mechanical properties of silicon nitride ceramics with controlled porosity, J. Am. Ceram. Soc. 85 (2002) 1512–1516.
[17] N. Kondo, Y. Suzuki, High-strength porous silicon nitride fabricated by the sinter-forging technique, J. Mater. Res. 16 (2001) 32–34.
[18] J.F. Yang, Z.Y. Deng, Fabrication and characterisation of porous silicon nitride ceramics using Yb_2O_3 as sintering additive, J. Eur. Ceram. Soc. 23 (2003) 371–378.
[19] J. She, J.F. Yang, Thermal shock behavior of isotropic and anisotropic porous silicon nitride, J. Am. Ceram. Soc. 86 (2003) 738–740.
[20] E. Sudhakar Reddy, J.G. Noudem, Open porous foam oxide thermoelectric elements for hot gases and liquid environments, Energy Convers. Manage. 48 (2007) 1251–1254.
[21] C.Y. Chu, J.P. Singh, High-temperature failure mechanisms of hot-pressed Si_3N_4 and Si_3N_4/Si_3N_4-whisker-reinforced composites, J. Am. Ceram. Soc. 76 (1993) 1349–1353.
[22] T. Kusunose, R. Sung, High-temperature properties of a silicon nitride/boron nitride nanocomposites, J. Mater. Res. 19 (2004) 1432–1438.